Engineering inducible signaling receptors to enable erythropoietin-free erythropoiesis

Aadit P. Shah[1,2]*, Kiran R. Majeti[2]*, Freja K. Ekman[1,2,3], Sridhar Selvaraj[2], Eric Soupene[4], Prathamesh Chati[5], Roshani Sinha[6,7], Sofia E. Luna[1,2], Carsten T. Charlesworth[3], Travis McCreary[6,7], Benjamin J. Lesch[6,7], Tammy Tran[6,7], Devesh Sharma[6,7], Simon N. Chu[6,7], Matthew H. Porteus[2†], M. Kyle Cromer[6,7,8†]

Affiliations:

[1]School of Medicine, Stanford University, Stanford, CA, USA

[2]Department of Pediatrics, Stanford University, Stanford, CA, USA

[3]Department of Genetics, Stanford University, Stanford, CA, USA

[4]Benioff Children's Hospital Oakland, University of California, San Francisco, San Francisco, CA, USA

[5]Department of Biological & Medical Informatics, University of California, San Francisco, San Francisco, CA, USA

[6]Department of Surgery, University of California, San Francisco, San Francisco, CA, USA

[7]Eli & Edythe Broad Center for Regeneration Medicine, University of California, San Francisco, San Francisco, CA, USA

[8]Department of Bioengineering & Therapeutic Sciences, University of California, San Francisco, San Francisco, CA, USA

*These authors contributed equally to the study

[†]Correspondence: mporteus@stanford.edu, kyle.cromer@uscf.edu

Abstract

Blood transfusion plays a vital role in modern medicine. However, availability is contingent on donated blood, and frequent shortages pose a significant healthcare challenge. *Ex vivo* manufacturing of red blood cells (RBCs) derived from universal donor O-negative pluripotent stem cells emerges as a solution, yet the high cost of recombinant cytokines required for *ex vivo* erythroid differentiation remains a major barrier. Erythropoietin (EPO) signaling through the EPO receptor is indispensable to RBC development, and EPO is one of the most expensive

33 components in erythroid-promoting media. Here, we used design-build-test cycles to develop
34 highly optimized small molecule-inducible EPO receptors (iEPORs) which were integrated at a
35 variety of genomic loci using homology-directed repair genome editing. We found that
36 integration of iEPOR at the endogenous *EPOR* locus in an induced pluripotent stem cell
37 producer line enabled culture with small molecule to yield equivalent erythroid differentiation,
38 transcriptomic changes, and hemoglobin production compared to cells cultured with EPO. Due
39 to the dramatically lower cost of small molecules vs. recombinant cytokines, these efforts
40 eliminate one of the most expensive elements of *ex vivo* culture media—EPO cytokine. Because
41 dependence on cytokines is a common barrier to *ex vivo* cell production, these strategies could
42 improve scalable manufacturing of a wide variety of clinically relevant cell types. More broadly,
43 this work showcases how synthetic biology and genome editing may be combined to introduce
44 precisely regulated and tunable behavior into cells, an advancement which will pave the way for
45 increasingly sophisticated cell engineering strategies.
46
47
48 **Introduction**
49
50 Blood cell transfusion plays an essential role in modern medicine. In support of surgery,
51 obstetrics, trauma care, and cancer chemotherapy, approximately 35,000 units of blood are
52 drawn daily in the U.S., contributing to an annual provision of 12 million red blood cell (RBC)
53 units[1]. However, availability is contingent on donated blood, resulting in supply constraints and
54 safety concerns. Blood shortages pose a significant global healthcare challenge, expected to
55 worsen with aging populations and decreasing donor numbers[2]. Moreover, patient populations
56 with especially rare blood types constitute up to 5% of blood transfusion cases[3] and are most
57 vulnerable to these shortages. From a financial perspective, the cost of RBC transfusion has
58 been steadily increasing over the past two decades, accounting for nearly 10% of total inpatient
59 hospital expenditure[4]. Collectively, these factors are expected to worsen the significant unmet
60 medical need for transfusable blood.
61 To address these challenges, *ex vivo* manufacturing of RBCs in bioreactors from
62 producer cell lines, such as pluripotent stem cells (PSCs), emerges as a renewable and scalable
63 solution[5]. Early clinical trials have shown that *ex vivo*-derived RBCs may be delivered to patients
64 with no reported adverse events[6]. In addition, *ex vivo*-derived RBCs offer potential benefits

65 compared to donor blood, including a lower risk of infectious disease transmission, streamlined
66 production, product uniformity, and ability to source or genetically engineer antigen-negative
67 cells[2]. However, *ex vivo* RBC production is still prohibitively expensive, owing in large part to the
68 high cost of recombinant cytokines required to stimulate producer cells to expand and
69 differentiate into erythroid cells[7]. Erythropoietin (EPO) signaling through the EPO receptor
70 (EPOR) is indispensable to RBC development[8], and of all components in erythroid-promoting
71 media, EPO is one of the most expensive[7]. Given prior success manipulating the EPOR to
72 increase erythropoietic output[9] and the ease with which erythroid development is modeled *ex*
73 *vivo*[10], in this work we used synthetic biology tools and genome editing technology to de-
74 couple EPOR signaling from the EPO cytokine.

75 The cellular mechanisms that regulate erythroid differentiation from hematopoietic
76 stem and progenitor cells (HSPCs) are well understood, and efficient differentiation requires
77 activation of the EPOR/JAK/STAT signaling cascade by EPO[11]. In its native form, two EPOR
78 monomers dimerize in the presence of EPO to activate downstream signaling[12]. Prior work has
79 shown that EPOR dimerization may be initiated by a range of dimer orientations and
80 proximities using agonistic diabodies or in the context of chimeric receptors[12–14]. Because
81 mutant FK506 binding proteins (FKBP)-based dimerization domains have been deployed to
82 create small molecule-inducible safety switches[15], we hypothesized that FKBP domains could
83 be repurposed to create synthetic EPOR receptors to place EPO signaling under control of a
84 small molecule. Here, we demonstrate that EPOR signaling can be induced by small molecule
85 stimulation of highly optimized chimeric receptors—hereafter termed inducible EPORs
86 (iEPORs). We then used homology-directed repair genome editing to integrate these iEPORs
87 under regulation of various endogenous and exogenous promoters to identify strategies that
88 best recapitulate native EPOR signaling.

89 This work establishes iEPORs as a tool that enables highly efficient *ex vivo* production
90 of RBCs using a low-cost small molecule. By removing dependence on one of the most
91 expensive elements of *ex vivo* erythrocyte production, these efforts address one of the major
92 barriers to meeting the global demand for blood with *ex vivo*-manufactured RBCs. More
93 broadly, this work demonstrates how synthetic biology and genome editing may be combined
94 to introduce precisely regulated and tunable behavior into cells for a wide variety of therapeutic
95 applications.
96

97 **Results**

98

99 *FKBP-EPOR chimeras enable small molecule-dependent erythropoiesis*

100

101 To determine whether FKBP domains could be successfully repurposed to dimerize
102 EPOR monomers and initiate downstream EPOR signaling, we first designed a set of seven
103 candidate FKBP-EPOR chimeras. These included placement of the FKBP domain at the N-
104 terminus, C-terminus, at various locations within the native EPOR, and as a full replacement of
105 the EPOR extracellular domain (**Fig. 1A**). DNA donor templates corresponding to each design
106 were packaged in AAV6 vectors and integrated into the *CCR5* safe harbor site in human primary
107 HSPCs using combined CRISPR/AAV6-mediated genome as previously described[16–18].
108 Expression of each FKBP-EPOR chimera was driven by the strong, constitutive SFFV promoter
109 followed by a 2A-YFP to allow fluorescent readout of edited cells (**Fig. 1A**). Edited HSPCs were
110 then subjected to an established 14-day *ex vivo* erythrocyte differentiation protocol[19,20] in the
111 absence of EPO and with or without 1nM of FKBP dimerizer AP20187 small molecule (hereafter
112 referred to as "BB" dimerizer)[15]. Since EPO is essential for differentiation, we hypothesized that
113 erythroid differentiation would only occur when BB stimulated a functional iEPOR to activate
114 downstream signaling (**Fig. 1B**).

115 At the end of differentiation, we stained cells for established erythroid markers and
116 analyzed by flow cytometry (**Supplementary Fig. S1**). As expected, we found that unedited
117 "Mock" conditions yielded no erythroid cells ($CD34^-/CD45^-/CD71^+/GPA^+$), while HSPCs edited
118 with iEPOR designs 1.4 and 1.5 showed BB-dependent erythroid differentiation (**Fig. 1C;**
119 **Supplementary Fig. S2**). Although FKBP-EPOR design 1.4 appeared to be most effective, for
120 downstream optimizations we iterated on design 1.5 due to the smaller cassette size and
121 because removal of the entire EPOR extracellular domain is expected to eliminate potential
122 activation by EPO cytokine. This allowed us to create a receptor that could activate the EPOR
123 pathway only when dimerizer was present but not when endogenous hormone was present.
124 Further investigation of iEPOR 1.5 found a >4x selective advantage imparted to edited cells by
125 the end of erythroid differentiation when cells were cultured in the presence of BB without EPO
126 as indicated by increasing edited allele frequency measured by droplet digital PCR (ddPCR)(**Fig.**
127 **1D**). In addition, virtually all cells that acquired erythroid markers in the iEPOR 1.5 condition
128 were YFP^+ (**Fig. 1E**), indicating that only edited cells were capable of differentiation.

129 To investigate why certain FKBP-EPOR designs were non-functional, we used
130 AlphaFold2[21] to generate *in silico* structure predictions of each candidate iEPOR in comparison
131 to wild-type EPOR. We observed a high-confidence structure generated across wild-type EPOR
132 extracellular and transmembrane domains, with low-confidence scores given to signal peptide
133 and intracellular regions (**Supplementary Fig. S3**). For candidate iEPORs, we observed a high-
134 confidence structure corresponding to the FKBP domain at the anticipated location among all
135 designs. Although this analysis did not reveal any obvious protein structure disruption caused
136 by addition of FKBP domains to the EPOR protein, our experiments demonstrated that FKBP
137 placement within the EPOR has a great bearing on its signaling potential. We found that only
138 those constructs with FKBP placed immediately upstream of the EPOR transmembrane domain
139 could initiate BB-dependent signaling. Therefore, it is possible that designs with FKBP within
140 the intracellular domain may interfere with JAK/STAT signaling, while FKBPs placed further
141 upstream of the transmembrane domain may not mediate sufficient proximity of EPOR
142 intracellular domains to achieve sustained signaling.
143
144
145 *Signal peptides and hypermorphic EPOR mutation increase iEPOR potency*
146
147 Initial iEPOR designs 1.4 and 1.5 both mediated BB-dependent erythroid production,
148 yet they were unable to achieve a level of differentiation equivalent to unedited cells cultured
149 with EPO (mean of 78.9% and 32.2% of the amount of differentiation achieved with unedited
150 cells +EPO for iEPOR 1.4 and 1.5, respectively; **Fig. 1C**). Therefore, we engineered second-
151 generation iEPORs to determine if addition of a signal peptide (SP) onto iEPOR 1.5 could
152 enhance potency, since elimination of the entire EPOR extracellular domain also removes the
153 native SP at the N-terminus. To test the effect of these modifications, we designed and built
154 constructs that added the native EPOR SP or the IL6 SP[22] onto the N-terminus of iEPOR 1.5.
155 This comparison was performed because SPs for cytokines are known to be particularly
156 strong[23,24], and we observed in unpublished work that the IL6 SP effectively mediates export to
157 the HSPC membrane (data not shown). These DNA donor templates were packaged into AAV6
158 and integrated into the *CCR5* locus as before (**Fig. 2A**). We then performed *ex vivo* erythroid
159 differentiation in the presence or absence of EPO and BB. We found that addition of EPOR SP
160 and IL6 SP both improved mean erythroid differentiation in the presence of BB alone (44.5%

161 and 62.6%, respectively) compared to the original iEPOR 1.5 design (32.2%)(**Fig. 2B** &
162 **Supplementary Fig. S4**). These vectors also yielded a further selective advantage in the
163 presence of BB (both with and without EPO), achieving a mean 10.0- and 10.6-fold increase in
164 edited allele frequency by the end of erythroid differentiation with addition of EPOR and IL6
165 SPs, respectively (**Fig. 2C** & **Supplementary Fig. S5A**).

166 Given the higher efficacy of iEPOR 1.5 with IL6 SP, we investigated whether
167 incorporation of a naturally occurring nonsense mutation (*EPOR*^{W439X}) that truncates the 70 C-
168 terminal amino acids of EPOR and eliminates a negative inhibitory domain may additionally
169 increase receptor potency[9]. Therefore, we designed a vector with this truncated EPOR
170 intracellular domain as well as IL6 SP and observed a further enhancement, achieving a mean of
171 90.9% erythroid differentiation compared to EPO-cultured HSPCs (**Fig. 2B**). This significantly
172 increased the selective advantage of edited cells cultured in the presence of BB, achieving a
173 mean 11.9-fold increase in edited alleles by the end of erythroid differentiation (**Fig. 2C**). As
174 before, virtually all cells that acquired erythroid markers were YFP^{+}, indicating that only edited
175 cells stimulated with BB were able to initiate EPOR signaling (**Fig. 2D**). Notably, a substantial
176 portion of cells also differentiated in the absence of BB, which we addressed in downstream
177 experiments. We will hereafter refer to our optimized FKBP-EPOR design 1.5 with IL6 SP and
178 naturally occurring truncation as "iEPOR").

179 To ensure that iEPOR-stimulated erythroid cells produce functional hemoglobin, we
180 performed hemoglobin tetramer high-performance liquid chromatography (HPLC) at the end
181 of erythroid differentiation. We found that cells edited with the optimized iEPOR and cultured
182 with BB yielded a hemoglobin production profile consisting primarily of adult and fetal
183 hemoglobin (HbA and HbF, respectively). This hemoglobin production profile was
184 indistinguishable from that produced by unedited cells culture with EPO (**Fig. 2E**).

185 Finally, we used AlphaFold2 to predict the structure of the optimized iEPOR and find
186 remarkable similarity to the predicted structure of the naturally occurring truncated EPOR (**Fig.
187 2F**). As expected, we observe a shortening of the low-confidence intracellular domain for the
188 truncated EPOR compared to wild-type EPOR (**Supplementary Fig. S6**) as well as a high-
189 confidence structure corresponding to the FKBP domain in the expected location for the
190 optimized iEPOR. As with native EPOR SP, we also observe a low-confidence region
191 corresponding to the IL6 SP.
192

193

194 *iEPOR expression profile impacts receptor function*

195

196 While our optimized iEPOR was effective at mediating small molecule-dependent
197 erythroid differentiation and hemoglobin production, we observed some erythroid
198 differentiation and hemoglobin production in the absence of BB as well (**Fig. 2B-E**). This could
199 be due to the strong, constitutive viral SFFV promoter driving supraphysiologic levels of
200 receptor expression that induced ligand-independent dimerization. In contrast to the potent
201 SFFV promoter, prior work has shown that $CD34^+$ HSPCs express low levels of the endogenous
202 *EPOR*, and expression increases modestly over the course of *ex vivo* erythroid differentiation[25].
203 Therefore, in the next round of optimizations, we explored the impact of various expression
204 profiles on iEPOR activity. To do so, we developed targeted integration strategies that placed
205 an identical optimized iEPOR under expression from: 1) an exogenous yet weaker, constitutive
206 human *PGK1* promoter following integration at the *CCR5* locus (hereafter referred to as
207 "*PGK*(iEPOR)"); 2) the strong erythroid-specific *HBA1* promoter following integration into the
208 start codon of the *HBA1* locus[10] (hereafter referred to as "*HBA1*(iEPOR)"); and 3) the
209 endogenous *EPOR* locus following integration into the 3′ end of the gene and linked by a 2A
210 cleavage peptide (hereafter referred to as "*EPOR*(iEPOR)")(**Fig. 3A**). We chose these additional
211 integration strategies to investigate whether extremely high *iEPOR* expression or simply
212 constitutive expression throughout differentiation was most responsible for the dimerizer-
213 independent activity of SFFV(iEPOR). These experiments also investigated whether erythroid-
214 specific expression of iEPOR from the highly expressed *HBA1* locus may elicit the most
215 dramatic pro-erythroid effect or if, alternatively, integration of iEPOR at the endogenous *EPOR*
216 locus may best recapitulate native EPOR signaling—analogous to the effective regulation of
217 synthetic T cell receptors when knocked into the native *TRAC* locus[26].

218 Following integration of each vector into the intended site in primary HSPCs, we
219 performed *ex vivo* erythroid differentiation in presence or absence of EPO and BB. We observed
220 that all three integration strategies yielded effective erythroid differentiation in presence of BB
221 compared to unedited cells cultured with EPO (**Fig. 3B** & **C**). However, the greatest differences
222 were found in edited conditions cultured without BB or EPO. Compared to the mean 26.3%
223 erythroid differentiation we observed previously in the SFFV(iEPOR)-edited condition without
224 EPO or BB, expression of iEPOR from the *PGK* and *EPOR* promoters both reduced BB-

225 independent activity (mean of 2.2% and 20.0% in *PGK*(iEPOR) and *EPOR*(iEPOR) conditions,
226 respectively)(**Fig. 3B** & **C**). In contrast, we found that expression of iEPOR from the *HBA1*
227 promoter drove high frequencies of erythroid differentiation in the presence and absence of
228 BB, indicating constitutive activity (**Fig. 3B** & **C**). Because *HBA1* is expressed much more highly
229 than *EPOR* by the end of *ex vivo* differentiation[27], we hypothesize this BB-independent activity
230 could be a result of supraphysiologic levels of *iEPOR* expression from the *HBA1* promoter that
231 leads to spontaneous signaling even in absence of dimerizing ligand. As before, we confirmed
232 that each iEPOR integration strategy yielded normal production of adult and fetal hemoglobin
233 when edited cells were cultured in the presence of BB without EPO (**Fig. 3D**). Due to the high
234 level of erythroid differentiation observed in the *HBA1*(iEPOR) condition, it was unsurprising
235 that edited cells cultured with neither EPO nor BB also produced a substantial amount of adult
236 and fetal hemoglobin.
237 Next, we determined whether expression of *iEPOR* from these different promoters has
238 a bearing on the dose response to BB. While prior work using BB found 1nM to be most
239 effective at activating small molecule-inducible safety switches[15], we observed substantial
240 erythroid differentiation at levels well below 1nM of BB. In fact, we found that 1pM and 10pM of
241 BB yielded erythroid differentiation that was comparable to EPO in cells edited with
242 *EPOR*(iEPOR) and *PGK*(iEPOR) strategies, respectively (**Fig. 3E**). However, to achieve mean
243 differentiation that was identical to or greater than EPO-stimulated cells required a dose of
244 0.1nM for *PGK*(iEPOR)- and *EPOR*(iEPOR)-edited populations. In contrast, we found that cells
245 edited with *HBA1*(iEPOR) yielded efficient erythroid differentiation across the entire dose
246 range, including in the absence of BB (**Fig. 3E**), consistent with constitutive activity of this
247 integration strategy.
248
249
250 *iEPOR closely replicates native EPOR signaling*
251
252 In its native form, EPO cytokine dimerizes two EPOR monomers, leading to a JAK/STAT
253 signaling cascade culminating in translocation of phosphorylated STAT5 to the nucleus, which
254 initiates a pro-erythroid transcriptional program[11]. While we have shown that iEPOR-edited
255 cells stimulated with BB acquire classic erythroid markers and produce normal hemoglobin
256 profiles, an open question is whether this synthetic stimulus recapitulates the complex

257 transcriptional response of native EPOR signaling (**Fig. 4A**). To investigate this, we edited
258 HSPCs with our various iEPOR integration strategies (**Fig. 3A**) and performed bulk RNA-
259 sequencing (RNA-Seq) on at d14 of erythroid differentiation in absence of EPO and presence of
260 BB. For comparison, we also performed RNA-Seq on unedited cells at the beginning (do) and
261 end (d14) of erythroid differentiation in the presence of EPO. These efforts yielded an average
262 of 55.1M reads per sample with 98.5% of reads aligned to the genome and 97.2% with Quality
263 Score $\geq$20 (**Supplementary Fig. S7**).

264 In analyzing these data, we found that alpha-, gamma-, and beta-globin are among the
265 most significantly upregulated genes in unedited cells at d14 vs. do (**Fig. 4B** & **C**). Similarly for
266 all cells edited with iEPOR, these globins are also among the most significantly upregulated
267 genes (**Fig. 4B** & **C**). In fact, by the end of differentiation these globins comprise a mean of
268 86.5%, 76.9%, 63.3%, and 83.7% of all reads for unedited cells cultured with EPO as well as
269 *PGK*(iEPOR)-, *HBA1*(iEPOR), and *EPOR*(iEPOR)-edited cells cultured with BB, respectively
270 (**Supplementary Fig. S8A**). As previously observed, we found that *EPOR* expression increases
271 over the course of erythroid differentiation[25] (38.8-fold from do to d14 in unedited cells; **Fig. 4B**
272 & **Supplementary Fig. S8B**). In all iEPOR-edited cells we observe roughly equivalent levels of
273 *EPOR* compared to unedited cells, which is expected since each integration strategy preserves
274 native *EPOR* expression. As for *iEPOR* expression, we find that both *PGK* and *EPOR* promoters
275 drive expression comparable to that of native *EPOR* at d14 in unedited cells (**Fig. 4B** &
276 **Supplementary Fig. S8C**). However, the *HBA1* promoter drives supraphysiologic levels of
277 *iEPOR*, with expression nearing that of the globins. Since the *HBA1*(iEPOR) integration strategy
278 replaces a full copy of the *HBA1* gene with *iEPOR* transgene, it is not surprising to find a
279 significant decrease in *HBA1* expression in this condition as well (**Fig. 4B, Supplementary Fig.**
280 **S8A**, & **S8D**). Consistent across donors, genes most highly expressed in HSPCs are uniformly
281 downregulated in all d14 samples while erythroid-specific genes are uniformly upregulated
282 (**Fig. 4B, 4C**, & **Supplementary Fig. S8D-G**). Because of this, we find that do HSPCs and all d14
283 samples segregate into two distinct hierarchies (**Supplementary Fig. 9A**), indicating a high
284 degree of similarity across all d14 samples regardless of whether these were unedited cells
285 cultured with EPO or iEPOR-edited cells cultured with BB.

286 Although consistent differences were observed comparing all conditions to do HSPCs,
287 we next determined whether significant differences existed at the end of differentiation
288 between unedited cells cultured with EPO and iEPOR-edited conditions cultured with BB. This

289 comparison revealed an extremely high degree of similarity between unedited cells cultured
290 with EPO and *PGK*(iEPOR)-edited cells cultured with BB; only three genes were differentially
291 expressed, including upregulation of the *iEPOR* transgene (**Fig. 4D**). In contrast, the
292 transcriptome of *HBA1*(iEPOR)-edited cells departed more substantially from unedited cells,
293 with a total of 47 differentially expressed genes. As expected, in this condition we observed
294 significant upregulation of *iEPOR* as well as downregulation of *HBA1*. Remarkably, we find that
295 the only differentially expressed gene in *EPOR*(iEPOR)-edited conditions is the *iEPOR*
296 transgene, indicating that this condition best recapitulated native EPOR signaling. These
297 conclusions were further supported by principal component analysis, which found that all d14
298 samples clustered separately from d0 samples and that *EPOR*(iEPOR)-edited cells stimulated
299 with BB most closely resemble unedited cells cultured with EPO (**Fig. 4E**). Gene co-expression
300 network analysis additionally revealed a high degree of similarity between iEPOR-edited
301 conditions and unedited cells cultured with EPO (**Supplementary Fig. S9B**).
302 To determine which cellular processes were activated by EPO compared to edited cells
303 cultured with BB, we performed gene ontology analysis of differentially expressed genes in
304 each condition compared to unedited cells at d0 (**Fig. 4F**). At d14, the most highly enriched
305 pathways were hydrogen peroxide (H_2O_2) catabolism—a critical function of erythrocytes to
306 process the significant amounts of superoxide and H_2O_2 that occur during oxygen transport[28].
307 We also find gas transport and erythroid differentiation processes to be highly enriched across
308 all d14 samples. From this analysis, the *HBA1*(iEPOR) condition shows the most substantial
309 departure from native EPOR signaling, with a number of significantly enriched pathways
310 unrelated to erythrocyte function. On the other hand, we find that *EPOR*(iEPOR) most closely
311 resembles native EPOR signaling, leading us to conclude that expression of synthetic receptors
312 from the endogenous promoter is likely to best recapitulate the transcriptomic changes
313 initiated by native cytokine signaling.
314
315
316 *iEPOR enables EPO-free erythropoiesis from O-negative induced pluripotent stem cells*
317
318 All prior work was done in primary HSPCs to determine whether we could successfully
319 engineer small molecule-inducible EPORs that recapitulate native erythroid development and
320 function. However, while primary hematopoietic HSPCs may be sourced from umbilical cord

321 blood and mobilized peripheral blood to produce RBCs *ex vivo*, their expansion capacity is
322 limited[2]. As a solution, induced pluripotent stem cell (iPSC) producer lines provide a potentially
323 unlimited source of patient-derived RBCs[6]. Therefore, in downstream experiments we used an
324 iPSC line called PB005 derived from a healthy donor with O-negative blood type[29] to determine
325 if iEPORs could effectively produce erythroid cells from a "universal" blood donor.

326 To test this, we integrated our most effective *iEPOR* expression strategies—
327 *PGK*(iEPOR) and *EPOR*(iEPOR)—into the PB005 iPSC line and isolated homozygous knock-in
328 clones (**Fig. 5A** & **Supplementary Fig. S10A**). These clones were then subjected to an
329 established 12-day differentiation into hematopoietic progenitor cells (HPCs). Surprisingly, we
330 found that *EPOR*(iEPOR)-edited clones yielded a substantially greater total cell count
331 compared to both unedited and *PGK*(iEPOR)-edited clones (**Supplementary Fig. S10B**),
332 although this condition had a slightly higher proportion of cells staining for erythroid markers
333 (**Supplementary Fig. S10C & D**). Following iPSC-to-HPC differentiation, we performed a 14-
334 day RBC differentiation without EPO and +/-BB (**Fig. 5A**). We found that all cells (unedited and
335 edited) effectively differentiated in the presence of EPO, whereas no erythroid differentiation
336 was observed in unedited cells in the absence of EPO (**Fig. 5B** & **Supplementary Fig. S11A**).
337 *PGK*(iEPOR)-edited cells stimulated with BB yielded a high percentage of erythroid cells, but
338 differentiation efficiency was significantly less than that achieved by EPO in these clones at
339 every timepoint (**Fig. 5B**). In addition, overall cell proliferation was substantially lower than that
340 achieved with EPO (**Fig. 5C**). In contrast, *EPOR*(iEPOR) clones achieved a differentiation
341 efficiency that was indistinguishable from clones cultured with EPO; cell proliferation over the
342 course of differentiation was also nearly equivalent to that achieved with EPO (**Fig. 5B** & **C**).
343 Given frequent clonal differences observed in proliferation capacity, we also examined cell
344 proliferation from the best *PGK*(iEPOR)- and *EPOR*(iEPOR)-edited clones. By day 14, the most
345 highly proliferative *PGK*(iEPOR)-edited clone only achieved 37.3% of the proliferation of that
346 same clone when cultured with EPO (**Supplementary Fig. S11B**). However, the most effective
347 *EPOR*(iEPOR)-edited clone achieved even greater proliferation (107.8%) compared to the same
348 clone cultured with EPO.

349 Next, we measured the hemoglobin profiles of these iPSC-derived erythroid cells using
350 HPLC and observed fetal hemoglobin to be the most prevalent tetramer in the presence of
351 EPO, which is consistent with prior studies[30]. We found this to be the case as well for clones
352 edited with both *PGK*(iEPOR) and *EPOR*(iEPOR) conditions cultured with BB (**Fig. 5D**). While

353 *PGK*(iEPOR) conditions cultured with BB almost uniformly expressed lower fetal hemoglobin
354 than their EPO-cultured counterparts, we observed the opposite for *EPOR*(iEPOR)-edited
355 conditions, with clones cultured with BB typically producing elevated levels of fetal hemoglobin
356 relative to those same clones cultured with EPO (**Fig. 5D** & **E**). However, there appeared to be
357 some clonal variation since not all clones conformed to these trends (**Fig. 5E**). These findings
358 were further confirmed by quantifying hemoglobin production per cell, which was done using
359 HPLC to quantify the amount of heme released by hemoglobin based on a standard curve. This
360 analysis revealed generally elevated hemoglobin production across *EPOR*(iEPOR)-edited clones
361 cultured with BB compared to the same clones cultured with EPO (median of 33.1 vs. 24.4pg
362 hemoglobin per cell, respectively; **Supplementary Fig. S11C**). In contrast, clones edited with
363 *PGK*(iEPOR) showed higher hemoglobin production when cultured with EPO (median of 21.1
364 vs. 32.1pg hemoglobin per cell with BB vs. EPO, respectively). Importantly, these levels of
365 hemoglobin production are within the range expected for normal RBCs in the blood stream
366 (25.4-34.6pg/cell)[31,32]. We note that while transfused RBCs typically produce more HbA than
367 HbF, the healthy phenotype of patients with hereditary persistence of fetal hemoglobin (HPFH)
368 and the recent approval of Casgevy to induce high levels of HbF to treat sickle cell disease and
369 β-thalassemia provide support that a blood product with high HbF should be both safe and
370 effective[33,34].
371
372
373 **Discussion**
374
375 In this work we combined synthetic protein engineering with the specificity of
376 homology-directed repair genome editing to enable small molecule control of cell
377 differentiation and behavior. By first optimizing highly effective small molecule-responsive
378 receptors and then integrating them into endogenous regulatory machinery, we effectively
379 recapitulated native receptor signaling. These efforts enable cell signaling to be stimulated by
380 low-cost small molecules instead of recombinant cytokines currently required for *ex vivo* cell
381 manufacturing. In this specific instance, EPO is one of the most expensive components of
382 erythroid-promoting media[7]. Here, we demonstrate that *EPOR*(iEPOR)-edited cells cultured
383 with a small molecule are capable of achieving equivalent erythroid differentiation,
384 transcriptomic changes, and hemoglobin production compared to cells cultured with EPO. For

385 comparison, we determined the cost per mg of the largest commercially available units of
386 recombinant human EPO and AP20187 (BB) small molecule. We found that the price per mg of
387 BB was nearly 50-fold less than that of recombinant EPO (**Fig. 5F**). In addition, 1/10th the
388 amount of BB compared to recombinant EPO was required to yield equivalent erythroid
389 production from *EPOR*(iEPOR)-edited iPSCs. Taken together, the corresponding estimates for
390 cost of EPO required to produce a single unit of RBCs at a culture density of 5e7/mL is
391 $1,246.50, conversely the cost to produce an equivalent amount of RBCs using BB is $2.25.
392 While the tools and editing strategies defined in the work enable replacement of recombinant
393 EPO with low-cost small molecule, additional key advances must be achieved for *ex vivo* RBC
394 production to become biologically and economically feasible. These include further reducing
395 the cost of erythroid-promoting media, better replicating high-density RBC production that
396 occurs *in vivo*[30,35], and improving enucleation of adult hemoglobin-producing RBCs[36]. This is a
397 multi-faceted problem and will require sustained efforts to further reduce production expenses.
398 Nevertheless, by eliminating the requirement of EPO cytokine in erythroid-promoting media,
399 this work brings us one major step closer to establishing *ex vivo* RBC production as a scalable
400 and renewable source of blood cells for transfusion medicine.

401 More broadly, we envision a future where clinically relevant cell types may be
402 manufactured off-the-shelf and at scale to meet the broad spectrum of patient needs.
403 However, significant advances are needed to improve affordability and accessibility to patients.
404 Given the complexities of large-scale cell manufacturing, many innovations have been
405 accomplished by mechanical engineers who have developed improved bioreactors[30,37,38]. Our
406 work demonstrates how challenges within this space may also be addressed by genome
407 engineers to create more effective producer cells to seed these advanced bioreactors. Because
408 dependence on expensive cytokines is a common barrier to scalable production of any cells *ex*
409 *vivo*, the strategies defined in this work may be readily adapted to enable large-scale
410 production of platelets, neutrophils, T cells, and many other clinically relevant cell types. This
411 will ensure that advancements in cell engineering may be rapidly translated to patients at a cost
412 that is both affordable and accessible.

413 Finally, this work demonstrates the power of iterative design-build-test cycles to
414 rapidly improve function of synthetic proteins. In this work, test cycle 1 defined the ideal
415 placement of an FKBP domain within the EPO receptor. Test cycle 2 enhanced efficacy of
416 iEPOR designs by incorporation of signal peptides and a naturally occurring *EPOR* mutation.

417 Finally, test cycle 3 defined the ideal expression profile of our optimized iEPOR cassette when
418 placed under a variety of exogenous and endogenous promoters. Perhaps unsurprisingly, we
419 find that integration of the optimized iEPOR at the endogenous *EPOR* locus best recapitulates
420 native EPOR signaling, an engineering attribute enabled by homology-directed repair genome
421 editing. In addition, given the incredible modularity of membrane-bound receptors[39], it is
422 possible that the small molecule-inducible architecture defined in this work may inform the
423 design of other potentially useful small molecule-inducible receptors to modulate a wide
424 variety of cell signals. If so, it is likely that synthetic receptor function may be fine-tuned by
425 design-build-test cycles as well as genome editing to mediate precise integration into the
426 genome. Gaining precisely regulated and tunable control over cells will thus pave the way for
427 increasingly sophisticated cell engineering applications.
428
429
430 **Methods**
431
432 **Integration vector design**
433 Integration vectors were designed such that the left and right homology arms (LHA and RHA,
434 respectively) are immediately flanking the cut site in exon 2 of the *CCR5* locus or exon 8 of the
435 *EPOR* locus. For *HBA1* integration, full gene replacement was achieved as previously
436 described[10] using split homology arms—the LHA corresponding to the region immediately
437 upstream of the start codon and RHA corresponding to the region immediately downstream of
438 the cut site in the 3′ UTR of the *HBA1* gene. Homology arm length ranged from 400-1000bp. For
439 FKBP-EPOR chimeras, flexible GGGGS linkers were added between FKBP domains and SPs and
440 the *EPOR* gene. When placing the FKBP domain immediately adjacent to the EPOR
441 transmembrane domain, the TM domain was defined as amino acid sequence
442 PLILTLSLILVVILVLLTVLALLSH. EPOR SP was defined as amino acid sequence
443 MDHLGASLWPQVGSLCLLLAGAAW. IL6 SP was defined as amino acid sequence
444 MNSFSTSAFGPVAFSLGLLLVLPAAFPAP. The FKBP sequence used corresponded to amino
445 acid sequence
446 MLEGVQVETISPGDGRTFPKRGQTCVVHYTGMLEDGKKVDSSRDRNKPFKFMLGKQEVIRGWEE
447 GVAQMSVGQRAKLTISPDYAYGATGHPGIIPPHATLVFDVELLKLE. Finally, to avoid the
448 possibility of unintended recombination of iEPOR with the endogenous locus for *EPOR*(iEPOR)-

449 edited conditions, we disguised homology of iEPOR by creating silent mutations within the
450 *EPOR* domains at every possible codon, with a preference for codons that occurred more
451 frequently throughout the human genome[40]. All custom sequences for cloning were ordered
452 from Integrated DNA Technologies (IDT; Coralville, Iowa, USA). Gibson Assembly MasterMix
453 (New England Biolabs, Ipswich, MA, USA) was used for the creation of each vector as per the
454 manufacturer's instructions.
455
456 **AAV6 DNA repair template production & purification**
457 All AAV6 vectors were cloned into the pAAV-MCS plasmid (Agilent Technologies, Hayward, CA,
458 USA), which contains inverted terminal repeats (ITRs) derived from AAV2. To produce AAV6
459 vectors, we seeded HEK293T cells (Life Technologies, South San Francisco, CA, USA) in 2-5
460 15cm^2 dishes at 13-15×10^6 cells per plate; 24h later, each dish was transfected using 112µg
461 polyethyleneimine, 6µg of ITR-containing plasmid, and 22µg of pDGM6 (gift from D. Russell,
462 University of Washington), which contains the AAV6 cap genes, AAV2 rep genes, and Ad5
463 helper genes. After 48-72h of incubation, cells were collected and AAV6 capsids were isolated
464 using the AAVPro Purification Kit (All Serotypes, Takara Bio, San Jose, USA), as per the
465 manufacturer's instructions. AAV6 vectors were titered using a Bio-Rad QX200 ddPCR machine
466 and QuantaSoft software (v.1.7, Bio-Rad, Hercules, CA, USA) to measure the number of vector
467 genomes as described previously[10].
468
469 **HSPC culture**
470 Human CD34$^+$ HSPCs were cultured as previously described[10]. CD34$^+$ HSPCs were sourced from
471 fresh cord blood (generously provided by the Stanford Binns Family Program for Cord Blood
472 Research) and Plerixafor- and/or G-CSF-mobilized peripheral blood (AllCells, Alameda, CA, USA
473 or STEMCELL Technologies, Vancouver, Canada). CD34$^+$ HSPCs were cultured at 1-5×10^5
474 cells/mL in StemSpan SFEMII (STEMCELL Technologies) or Good Manufacturing Practice Stem
475 Cell Growth Medium (SCGM, CellGenix, Freiburg, Germany) base medium supplemented with a
476 human cytokine (PeproTech, Rocky Hill, NJ, USA) cocktail: stem cell factor (100ng/mL),
477 thrombopoietin (100ng/mL), Fms-like tyrosine kinase 3 ligand (100 ng/ml), interleukin-6
478 (100ng/mL), streptomycin (20mg/mL)(ThermoFisher Scientific, Waltham, MA, USA), and
479 penicillin (20U/mL)(ThermoFisher Scientific, Waltham, MA, USA), and 35nM of UM171 (cat.:

480 A89505; APExBIO, Houston, TX, USA). The cell incubator conditions were 37°C, 5% CO_2, and
481 5% O_2.
482
483 **Genome editing of HSPCs**
484 Chemically modified CRISPR guide RNAs (gRNAs) used to edit $CD34^+$ HSPCs at *CCR5*, *HBA1*,
485 and *EPOR* were purchased from Synthego (Redwood City, CA, USA). The gRNA modifications
486 added were 2′-O-methyl-3′-phosphorothioate at the three terminal nucleotides of the 5′ and 3′
487 ends, as described previously[41]. The target sequences for gRNAs were as follows: *CCR5*: 5′-
488 GCAGCATAGTGAGCCCAGAA-3′; *HBA1*: 5′-GGCAAGAAGCATGGCCACCGAGG-3′; and *EPOR*:
489 5′-AGCTCAGGGCACAGTGTCCA-3′. All Cas9 protein was purchased from Aldevron (Alt-R S.p.
490 Cas9 Nuclease V3; Fargo, ND, USA). Cas9 ribonucleoprotein (RNP) complexes were created at a
491 Cas9/gRNA molar ratio of 1:2.5 at 25°C for a minimum of 10mins before electroporation. $CD34^+$
492 cells were resuspended in P3 buffer plus supplement (cat.: V4XP-3032; Lonza Bioscience,
493 Walkersville, MD, USA) with complexed RNPs and electroporated using the Lonza 4D
494 Nucleofector (program DZ-100). Cells were plated at 1-2.5×10^5 cells/mL following
495 electroporation in the cytokine-supplemented media described previously. Immediately
496 following electroporation, AAV6 was supplied to the cells at between 2.5-5e3 vector genomes
497 per cell. The small molecule AZD-7648, a DNA-dependent protein kinase catalytic subunit
498 inhibitor, was also added to cells immediately post-editing for 24h at 0.5nM to improve
499 homology-directed repair frequencies as previously reported[42].
500
501 ***Ex vivo* erythroid differentiation**
502 Following editing, HSPCs derived from healthy patients or iPSC-derived HPCs were cultured for
503 14d at 37°C and 5% CO_2 in SFEMII medium (STEMCELL Technologies, Vancouver, Canada) as
504 previously described[19,20]. SFEMII base medium was supplemented with 100U/mL
505 penicillin/streptomycin (ThermoFisher Scientific, Waltham, MA, USA), 10ng/mL stem cell factor
506 (PeproTech, Rocky Hill, NJ, USA), 1ng/mL interleukin-3 (PeproTech, Rocky Hill, NJ, USA),
507 3U/mL EPO (eBiosciences, San Diego, CA, USA), 200µg/mL transferrin (Sigma-Aldrich, St.
508 Louis, MO, USA), 3% antibody serum (heat-inactivated; Sigma-Aldrich), 2% human plasma
509 (isolated from umbilical cord blood provided by Stanford Binns Cord Blood Program), 10µg/mL
510 insulin (Sigma-Aldrich), and 3U/mL heparin (Sigma-Aldrich). In the first phase, at days 0–7 of
511 differentiation (day 0 being 2-3d post editing), cells were cultured at 1×10^5 cells/mL. In the

512 second phase (days 7–10), cells were maintained at 1×10^5 cells/mL and IL-3 was removed from
513 the culture. In the third phase (days 11–14), cells were cultured at 1×10^6 cells/mL and transferrin
514 was increased to 1mg/mL. For -EPO conditions, cells were cultured in the same culture medium
515 as listed above except for the removal of EPO from the media. For conditions with the addition
516 of BB homodimerizer (AP20187)(Takara Bio, San Jose, USA), 1µL of 0.5mM BB was diluted in
517 999µL PBS (HI30; BD Biosciences, San Jose, CA, USA), of which 2µL of the dilution was added
518 for every 1mL of differentiation media to reach a desired concentration of 1nM. Fresh BB was
519 added at each media change (Day 0, 4, 7, 11). For experiments requiring additional dilutions, BB
520 was diluted further in PBS to reach the required concentration (as low as 1pM).
521
522 **Immunophenotyping of differentiated erythrocytes**
523 HSPCs subjected to erythroid differentiation were analyzed at d14 for erythrocyte lineage-
524 specific markers using a FACS Aria II and FACS Diva software (v.8.0.3; BD Biosciences, San Jose,
525 CA, USA). Edited and unedited cells were analyzed by flow cytometry using the following
526 antibodies: hCD45 V450 (1:50 dilution; 2µl in 100µl of pelleted RBCs in 1×PBS buffer; HI30; BD
527 Biosciences), CD34 APC (1:50 dilution; 561; BioLegend, San Diego, CA, USA), CD71 PE-Cy7
528 (1:500 dilution; OKT9; Affymetrix, Santa Clara, CA, USA), and CD235a PE (GPA)(1:500 dilution;
529 GA-R2; BD Biosciences). In addition to cell-specific markers, cells were also stained with Ghost
530 Dye Red 780 (Tonbo Biosciences, San Diego, CA, USA) to measure viability.
531
532 **Editing frequency analysis**
533 Between 2-4d post editing, HSPCs were harvested and QuickExtract DNA extraction solution
534 (Epicentre, Madison, WI, USA) was used to collect genomic DNA (gDNA). Additional samples
535 were collected at various stages of differentiation (d4, 7, 11, and 14 of erythroid differentiation)
536 gDNA was then digested using BamH1-HF as per the manufacturer's instructions (New England
537 Biolabs, Ipswich, MA, USA). Percentage of targeted alleles within a cell population was
538 measured with a Bio-Rad QX200 ddPCR machine and QuantaSoft software (v.1.7; Bio-Rad,
539 Hercules, CA, USA) using the following reaction mixture: 1-4µL of digested gDNA input, 10µL
540 of ddPCR SuperMix for Probes (no dUTP)(Bio-Rad), primer/probes (1:3.6 ratio; Integrated DNA
541 Technologies, Coralville, IA, USA) and volume up to 20µL with H_2O. ddPCR droplets were then
542 generated following the manufacturer's instructions (Bio-Rad): 20µL of ddPCR reaction, 70µL
543 of droplet generation oil, and 40µL of droplet sample. Thermocycler (Bio-Rad) settings were as

544 follows: 98°C (10mins), 94°C (30s), 57.3°C (30s), 72°C (1.75mins)(return to step 2×40-50 cycles),
545 and 98°C (10mins). Analysis of droplet samples was performed using the QX200 Droplet Digital
546 PCR System (Bio-Rad). To determine percentages of alleles targeted, the numbers of Poisson-
547 corrected integrant copies/mL were divided by the numbers of reference DNA copies/mL. The
548 following primers and 6-FAM/ZEN/IBFQ-labeled hydrolysis probes were purchased as custom-
549 designed PrimeTime quantitative PCR (qPCR) assays from Integrated DNA Technologies: All
550 *HBA1* vectors: forward: 5′-AGTCCAAGCTGAGCAAAGA-3′, reverse: 5′-
551 ATCACAAACGCAGGCAGAG-3′, probe: 5′-CGAGAAGCGCGATCACATGGTCCTGC-3′; all *CCR5*
552 vectors: forward: 5′-GGGAGGATTGGGAAGACAAT-3′, reverse: 5′-
553 TGTAGGGAGCCCAGAAGAGA-3′, probe: 5′-CACAGGGCTGTGAGGCTTAT-3′. The primers and
554 HEX/ZEN/IBFQ-labeled hydrolysis probe, purchased as custom-designed PrimeTime qPCR
555 Assays from Integrated DNA Technologies, were used to amplify the *CCRL2* reference gene:
556 forward: 5′-GCTGTATGAATCCAGGTCC-3′, reverse: 5′-CCTCCTGGCTGAGAAAAAG-3′, probe:
557 5′-TGTTTCCTCCAGGATAAGGCAGCTGT-3′.
558
559 **AlphaFold2 structural predictions**
560 Energy-predicted structures were derived by applying AlphaFold2 (v2.3.2)[21] on wild-type EPOR,
561 truncated EPOR, and iEPOR sequences. Five differently trained neural networks were applied
562 to produce unrelaxed structure predictions. Energy minimization was applied to the best
563 predicted unrelaxed structure (highest average highest average predicted distance difference
564 test (pLDDT) and lowest predicted aligned error) to produce the optimal relaxed structure.
565
566 **Hemoglobin tetramer analysis**
567 Frozen pellets of approximately 1×10^6 cells *ex vivo*-differentiated erythroid cells were thawed
568 and lysed in 30µL of RIPA buffer with 1x Halt Protease Inhibitor Cocktail (ThermoFisher
569 Scientific, Waltham, MA, USA) for 5mins on ice. The mixture was vigorously vortexed and cell
570 debris was removed by centrifugation at 13,000 RPM for 10mins at 4°C. HPLC analysis of
571 hemoglobins in their native form was performed on a cation-exchange PolyCAT A column (35 ×
572 4.6mm^2, 3µm, 1,500Å)(PolyLC Inc., Columbia, MD, USA) using a Perkin-Elmer Flexar HPLC
573 system (Perkin-Elmer, Waltham, MA, USA) at room temperature and detection at 415nm.
574 Mobile phase A consisted of 20mM Bis-tris and 2mM KCN at pH 6.94, adjusted with HCl. Mobile
575 phase B consisted of 20mM Bis-tris, 2mM KCN, and 200mM NaCl at pH 6.55. Hemolysate was

576 diluted in buffer A prior to injection of 20µL onto the column with 8% buffer B and eluted at a
577 flow rate of 2 mL/min with a gradient made to 40% B in 6mins, increased to 100% B in 1.5mins,
578 returned to 8% B in 1min, and equilibrated for 3.5mins. Quantification of the area under the
579 curve of peaks was performed with TotalChrom software (Perkin-Elmer) and raw values were
580 exported to GraphPad Prism software (v9) for plotting and further analysis.
581
582 **Bulk RNA-sequencing**
583 Total RNA was extracted from frozen pellets of approximately 1×10^6 cells per condition using
584 RNeasy Plus Micro Kit (Qiagen, Redwood City, CA, USA) according to the manufacturer's
585 instructions. Sequencing was provided by Novogene (Sacramento, CA, USA) and raw FASTQ
586 files were aligned to the GRCh38 reference genome extended with the iEPOR target sequence
587 and quantified using Salmon (v1.9.0)[43] with default parameters. Quality control was performed
588 by Novogene.
589
590 **Differential gene expression analysis & gene set enrichment analysis**
591 The estimated gene expression counts were used with DESeq2[44] to conduct differential gene
592 expression analysis between sample groups. Mitochondrial and lowly expressed genes were
593 removed (sum NumReads <1). The top 50 up- and down-regulated genes based on adjusted p-
594 value were isolated and analyzed with Enrichr[45] to yield functional annotations.
595
596 **Principal component analysis & gene distribution plots**
597 Mitochondrial genes were removed from the gene expression matrix (TPM) and the remaining
598 genes were used to conduct principal component analysis with all samples. Gene expression for
599 experimental and control groups were averaged and log-normalized. Average gene expression
600 distributions were plotted using Seaborn
601 (https://github.com/atsumiando/RNAseq_figure_plotter_python).
602
603 **Gene co-expression network analysis**
604 The TPM-normalized gene expression matrix of all *PGK*(iEPOR)-, *HBA1*(iEPOR)-, and
605 *EPOR*(iEPOR)-edited conditions (n=10) was used to construct a pairwise gene similarity matrix
606 where each entry represented the Spearman correlation coefficient between a pair of genes.
607 The correlation between a specified set of *EPOR*-related genes was compared for both *EPOR*

608 and *iEPOR* to determine which genes *iEPOR* adequately mimics in the immediate gene co-
609 expression network of native *EPOR*.
610
611 **iPSC line & culture**
612 A previously published iPSC line, PB005 derived from peripheral blood of a donor with O^- blood
613 type was used in this study[46]. iPSCs were cultured and maintained in mTeSR1 medium (cat.:
614 85850; STEMCELL Technologies, Vancouver, Canada) on Matrigel (cat.: 354277; Corning, NY,
615 USA)-coated plates. For passaging, cells at a confluency of 80-90% were incubated with
616 Accutase (cat.: AT104; Innovative Cell Technologies, San Diego, USA) for 5-7mins to dissociate
617 into single cells and replated in mTeSR1 medium supplemented with 10mM of ROCKi (Y27632;
618 cat.: 10005583; Cayman Chemical, Ann Arbor, MI, USA). After 24h, cells were maintained in
619 fresh mTeSR1 medium with daily media changes. For freezing iPS cells, STEM-CELLBANKER
620 freezing medium (cat.: 11924; Amsbio, Cambridge, MA, USA) was used.
621
622 **Genome editing of iPSCs**
623 iPSCs were genome edited using the CRISPR/AAV platform as described previously[17,42]. Cas9
624 RNP complex was formed by combining 5µg of Cas9 (Alt-R S.p. Cas9 Nuclease V3; Fargo, ND,
625 USA) and 2µg of gRNA (Synthego, Redwood City, CA, USA) and incubating at room
626 temperature for 15mins. iPSCs pre-treated with ROCKi (Y27632; cat.: 10005583; Cayman
627 Chemical, Ann Arbor, MI, USA) for 24 hours were dissociated with Accutase (cat.: AT104;
628 Innovative Cell Technologies, San Diego, USA) into single cells. $1\text{-}5\times10^5$ iPSCs were
629 resuspended in 20µL of P3 primary cell nucleofector solution plus supplement (cat.: V4XP-3032;
630 Lonza Bioscience, Walkersville, MD, USA) along with the RNP complex and nucleofected using
631 Lonza 4D Nucleofector (program CA-137). After nucleofection, iPSCs were plated in mTeSR1
632 medium supplemented with ROCKi, 0.25µM AZD7648 (cat.: S8843; Selleck Chemicals,
633 Houston, TX, USA) and AAV6 donor at 2.5×10^3 vector genomes per cell, based on ddPCR titers
634 as above. After 24h, cells were switched to medium with mTeSR1 and ROCKi. From the
635 following day, cells were maintained in mTeSR1 medium without ROCKi.
636
637 **Single-cell cloning of iPSCs**
638 To isolate single cell clones, genome-edited iPSCs were plated at a density of 250 cells per well
639 of a 6-well plate in mTeSR1 medium supplemented with 1x CloneR2 reagent (cat.: 100-0691;

640 STEMCELL Technologies, Vancouver, Canada). After 48h, cells were switched to fresh mTeSR1
641 medium with 1x CloneR2 and incubated for 2d. Following this, iPSCs were maintained in
642 mTeSR1 medium without CloneR2 with daily media changes. At d7-10, single cell colonies were
643 picked by scraping and propagated individually. The isolated single cell iPSCs were genotyped
644 using PCR with primers annealing outside the homology arms to identify clones with bi-allelic
645 knock-in. The following primers were used for genotyping: *CCR5* integration: forward: 5′-
646 CTCATAGTGCATGTTCTTTGTGGGC-3′, reverse: 5′-CCAGCCCAGGCTGTGTATGAAA-3′; *EPOR*
647 integration: forward: 5′-GCCACATGGCTAGAGTGGTAT-3′, reverse: 5′-
648 CTTTCTTAGAACATGGCCTGATTCAGA-3′.
649
650 **iPSC-to-erythrocyte differentiation**
651 iPSCs were differentiated into $CD34^+$ HPCs using the STEMdiff Hematopoietic Kit (cat.: 05310;
652 STEMCELL Technologies, Vancouver, Canada) according to the manufacturer's protocol.
653 Briefly, iPSCs at 70-80% confluency were dissociated into aggregates using ReLeSR (cat.: 100-
654 0484; STEMCELL Technologies). Aggregates were then diluted 10-fold, and 100µL of the
655 diluted suspension was aliquoted into a 96-well plate for quantification. Approximately 80
656 aggregate colonies were subsequently plated per well of a 12-well plate pre-coated with
657 Matrigel and maintained in mTeSR1 medium. 24h post-plating, the number of colonies per well
658 was manually quantified, and the medium was replaced with differentiation medium A. The
659 medium was then changed according to the kit's instructions for a total of 12 days. On d12,
660 suspension cells were harvested by pipetting cells up and down to ensure a homogeneous cell
661 suspension. To assess the efficiency of differentiation, as determined by $CD34^+/CD45^+$
662 expression, cells were analyzed using flow cytometry with the erythrocyte flow panel previously
663 described for HSPCs. Following this, $CD34^+$ cells were further differentiated into erythroid cells
664 using the three-phase system described above, either in the presence or absence of EPO and
665 BB.
666
667 **Heme detection analysis**
668 Quantification of the amount of hemoglobin produced in cells was obtained by quantitative
669 detection of the heme peak released from hemoglobin. Lysate were obtained from $1\text{-}2\times10^5$ cells
670 as frozen pellets, as described for hemoglobin tetramer analysis. The relationship between
671 heme and hemoglobin was established from serially diluted hemolysate made with a blood

sample of a known hemoglobin content. Detection of heme was performed by reverse-phase PerkinElmer Flexar HPLC system (PerkinElmer) with a Symmetry C18 column (4.6 × 75mm, 3.5µm; Waters Corporation, Milford, MA, USA) at 415nm. Mobile phase A consisted of 10% methanol made in acetonitrile and mobile B of 0.5% trifluoroacetic acid in water adjusted at pH 2.9 with NaOH. Samples were injected at a flow rate of 2mL/min in 49% A, followed by a 3min gradient to 100% A. The column was then equilibrated to 49% A for 3mins.

Statistical analysis

All statistical tests on experimental groups were done using GraphPad Prism software (v9). The exact statistical tests used for each comparison are noted in the individual figure legends.

Data availability

RNA-seq data will be uploaded to the NCBI Sequence Read Archive submission. The filtered data for all figures in this study are provided in the Extended Data.

Conflicts of interest

M.H.P. is a member of the scientific advisory board of Allogene Therapeutics. M.H.P. has equity in CRISPR Tx and Kamau Tx. C.T.C., M.H.P., and M.K.C. have filed provisional patent no. PCT/US2023/076969.

Acknowledgements

The authors thank the following funding sources that made this work possible: Stanford Medical Scholars Research Program, the American Society of Hematology Minority Medical Student Award Program, and the Stanford Medical Scientist Training Program to S.E.L.; National Science Foundation Graduate Research Fellowship Program to B.J.L.; University of California, San Francisco NIH T32 Research Training in Transplant Surgery Fellowship to S.N.C.; University of California, San Francisco Program for Breakthrough Biomedical Research: New Frontier Research Award to M.K.C; and Mary Anne Koda-Kimble Seed Award for Innovation to M.K.C. We also would also like to thank the Stanford Binns Program for Cord Blood Research

704 for providing $CD34^+$ HSPCs and the FACS Core Facility at the Stanford Institute of Stem Cell
705 Biology and Regenerative Medicine as well as University of California, San Francisco Flow Core
706 for access to flow cytometry machines. Finally, we would like to thank Caleb Grossman for
707 helpful discussions and feedback as we planned initial experiments.
708
709
710 **References**
711

712 1. Klein, H. G., Hrouda, J. C. & Epstein, J. S. Crisis in the sustainability of the U.S. blood system. *N.*
713 *Engl. J. Med.* **377,** 1485–1488 (2017).

714 2. Trakarnsanga, K. *et al.* An immortalized adult human erythroid line facilitates sustainable and
715 scalable generation of functional red cells. *Nat. Commun.* **8,** 14750 (2017).

716 3. Campbell-Lee, S. A. & Kittles, R. A. Red blood cell alloimmunization in sickle cell disease: listen
717 to your ancestors. *Transfus. Med. Hemother.* **41,** 431–435 (2014).

718 4. Trentino, K. M. *et al.* Increased hospital costs associated with red blood cell transfusion.
719 *Transfusion* **55,** 1082–1089 (2015).

720 5. Giarratana, M.-C. *et al.* Ex vivo generation of fully mature human red blood cells from
721 hematopoietic stem cells. *Nat. Biotechnol.* **23,** 69–74 (2005).

722 6. Giarratana, M.-C. *et al.* Proof of principle for transfusion of in vitro-generated red blood cells.
723 *Blood* **118,** 5071–5079 (2011).

724 7. Timmins, N. E. & Nielsen, L. K. Blood cell manufacture: current methods and future challenges.
725 *Trends Biotechnol.* **27,** 415–422 (2009).

726 8. Suzuki, N. *et al.* Erythroid-specific expression of the erythropoietin receptor rescued its null
727 mutant mice from lethality. *Blood* **100**, 2279–2288 (2002).

728 9. Camarena, J. *et al.* Using human genetics to develop strategies to increase erythropoietic output
729 from genome-edited hematopoietic stem and progenitor cells. *BioRxiv* (2023)
730 doi:10.1101/2023.08.04.552064.

731 10. Cromer, M. K. *et al.* Gene replacement of α-globin with β-globin restores hemoglobin balance in
732 β-thalassemia-derived hematopoietic stem and progenitor cells. *Nat. Med.* **27**, 677–687 (2021).

733 11. Mohan, K. *et al.* Topological control of cytokine receptor signaling induces differential effects in
734 hematopoiesis. *Science* **364**, (2019).

735 12. Moraga, I. *et al.* Tuning cytokine receptor signaling by re-orienting dimer geometry with
736 surrogate ligands. *Cell* **160**, 1196–1208 (2015).

737 13. Ohashi, H., Maruyama, K., Liu, Y. C. & Yoshimura, A. Ligand-induced activation of chimeric
738 receptors between the erythropoietin receptor and receptor tyrosine kinases. *Proc Natl Acad Sci*
739 *USA* **91**, 158–162 (1994).

740 14. Muthukumaran, G., Kotenko, S., Donnelly, R., Ihle, J. N. & Pestka, S. Chimeric erythropoietin-
741 interferon gamma receptors reveal differences in functional architecture of intracellular domains
742 for signal transduction. *J. Biol. Chem.* **272**, 4993–4999 (1997).

743 15. Martin, R. M. *et al.* Improving the safety of human pluripotent stem cell therapies using genome-
744 edited orthogonal safeguards. *Nat. Commun.* **11**, 2713 (2020).

745 16. Charlesworth, C. T. *et al.* Priming human repopulating hematopoietic stem and progenitor cells
746 for cas9/sgrna gene targeting. *Mol. Ther. Nucleic Acids* **12**, 89–104 (2018).

747 17. Martin, R. M. *et al.* Highly Efficient and Marker-free Genome Editing of Human Pluripotent Stem
748 Cells by CRISPR-Cas9 RNP and AAV6 Donor-Mediated Homologous Recombination. *Cell Stem*
749 *Cell* **24,** 821-828.e5 (2019).

750 18. Scharenberg, S. G. *et al.* Engineering monocyte/macrophage-specific glucocerebrosidase
751 expression in human hematopoietic stem cells using genome editing. *Nat. Commun.* **11,** 3327
752 (2020).

753 19. Dulmovits, B. M. *et al.* Pomalidomide reverses γ-globin silencing through the transcriptional
754 reprogramming of adult hematopoietic progenitors. *Blood* **127,** 1481–1492 (2016).

755 20. Hu, J. *et al.* Isolation and functional characterization of human erythroblasts at distinct stages:
756 implications for understanding of normal and disordered erythropoiesis in vivo. *Blood* **121,** 3246–
757 3253 (2013).

758 21. Yang, Z., Zeng, X., Zhao, Y. & Chen, R. AlphaFold2 and its applications in the fields of biology
759 and medicine. *Signal Transduct. Target. Ther.* **8,** 115 (2023).

760 22. Adam, N. *et al.* Unraveling viral interleukin-6 binding to gp130 and activation of STAT-signaling
761 pathways independently of the interleukin-6 receptor. *J. Virol.* **83,** 5117–5126 (2009).

762 23. Duitman, E. H., Orinska, Z., Bulanova, E., Paus, R. & Bulfone-Paus, S. How a cytokine is
763 chaperoned through the secretory pathway by complexing with its own receptor: lessons from
764 interleukin-15 (IL-15)/IL-15 receptor alpha. *Mol. Cell. Biol.* **28,** 4851–4861 (2008).

765 24. Figueiredo Neto, M. & Figueiredo, M. L. Skeletal muscle signal peptide optimization for
766 enhancing propeptide or cytokine secretion. *J. Theor. Biol.* **409,** 11–17 (2016).

767 25. Forejtnikovà, H. *et al.* Transferrin receptor 2 is a component of the erythropoietin receptor
768 complex and is required for efficient erythropoiesis. *Blood* **116,** 5357–5367 (2010).

769 26. Eyquem, J. *et al.* Targeting a CAR to the TRAC locus with CRISPR/Cas9 enhances tumour
770 rejection. *Nature* **543,** 113–117 (2017).

771 27. Chu, S. N. *et al.* Dual α-globin and truncated erythropoietin receptor knock-in restores
772 hemoglobin production in α-thalassemia major-derived hematopoietic stem and progenitor
773 cells. *BioRxiv* (2023) doi:10.1101/2023.09.01.555926.

774 28. Scott, M. D., Lubin, B. H., Zuo, L. & Kuypers, F. A. Erythrocyte defense against hydrogen
775 peroxide: preeminent importance of catalase. *J. Lab. Clin. Med.* **118,** 7–16 (1991).

776 29. Masaki, H. *et al.* Interspecific in vitro assay for the chimera-forming ability of human pluripotent
777 stem cells. *Development* **142,** 3222–3230 (2015).

778 30. Yu, S. *et al.* Selection of O-negative induced pluripotent stem cell clones for high-density red
779 blood cell production in a scalable perfusion bioreactor system. *Cell Prolif.* **55,** e13218 (2022).

780 31. Revin, V. V. *et al.* Study of Erythrocyte Indices, Erythrocyte Morphometric Indicators, and
781 Oxygen-Binding Properties of Hemoglobin Hematoporphyrin Patients with Cardiovascular
782 Diseases. *Adv. Hematol.* **2017,** 8964587 (2017).

783 32. Table 1, Complete blood count - Blood Groups and Red Cell Antigens - NCBI Bookshelf.
784 https://www.ncbi.nlm.nih.gov/books/NBK2263/table/ch1.T1/.

785 33. Forget, B. G. Molecular basis of hereditary persistence of fetal hemoglobin. *Ann. N. Y. Acad. Sci.*
786 **850,** 38–44 (1998).

787 34. Frangoul, H. *et al.* CRISPR-Cas9 Gene Editing for Sickle Cell Disease and β-Thalassemia. *N. Engl.*
788 *J. Med.* **384,** 252–260 (2021).

789 35. Sivalingam, J. *et al.* A Scalable Suspension Platform for Generating High-Density Cultures of
790 Universal Red Blood Cells from Human Induced Pluripotent Stem Cells. *Stem Cell Reports* **16,**
791 182–197 (2021).

792 36. Miharada, K., Hiroyama, T., Sudo, K., Nagasawa, T. & Nakamura, Y. Efficient enucleation of
793 erythroblasts differentiated in vitro from hematopoietic stem and progenitor cells. *Nat.*
794 *Biotechnol.* **24,** 1255–1256 (2006).

795 37. Bayley, R. *et al.* The productivity limit of manufacturing blood cell therapy in scalable stirred
796 bioreactors. *J. Tissue Eng. Regen. Med.* **12,** e368–e378 (2018).

797 38. Ahmed, S., Chauhan, V. M., Ghaemmaghami, A. M. & Aylott, J. W. New generation of
798 bioreactors that advance extracellular matrix modelling and tissue engineering. *Biotechnol. Lett.*
799 **41,** 1–25 (2019).

800 39. Bell, M. *et al.* Modular chimeric cytokine receptors with leucine zippers enhance the antitumour
801 activity of CAR T cells via JAK/STAT signalling. *Nat. Biomed. Eng.* (2023) doi:10.1038/s41551-023-
802 01143-w.

803 40. Tanida-Miyake, E., Koike, M., Uchiyama, Y. & Tanida, I. Optimization of mNeonGreen for Homo
804 sapiens increases its fluorescent intensity in mammalian cells. *PLoS ONE* **13,** e0191108 (2018).

805 41. Hendel, A. *et al.* Chemically modified guide RNAs enhance CRISPR-Cas genome editing in
806 human primary cells. *Nat. Biotechnol.* **33,** 985–989 (2015).

807 42. Selvaraj, S. *et al.* High-efficiency transgene integration by homology-directed repair in human
808 primary cells using DNA-PKcs inhibition. *Nat. Biotechnol.* (2023) doi:10.1038/s41587-023-01888-
809 4.

810 43. Patro, R., Duggal, G., Love, M. I., Irizarry, R. A. & Kingsford, C. Salmon provides fast and bias-
811 aware quantification of transcript expression. *Nat. Methods* **14,** 417–419 (2017).

812 44. Love, M. I., Huber, W. & Anders, S. Moderated estimation of fold change and dispersion for
813 RNA-seq data with DESeq2. *Genome Biol.* **15,** 550 (2014).

814 45. Kuleshov, M. V. *et al.* Enrichr: a comprehensive gene set enrichment analysis web server 2016
815 update. *Nucleic Acids Res.* **44,** W90-7 (2016).

816 46. Sun, S. *et al.* Human pluripotent stem cell-derived macrophages host Mycobacterium
817 abscessus infection. *Stem Cell Reports* (2022) doi:10.1016/j.stemcr.2022.07.013.

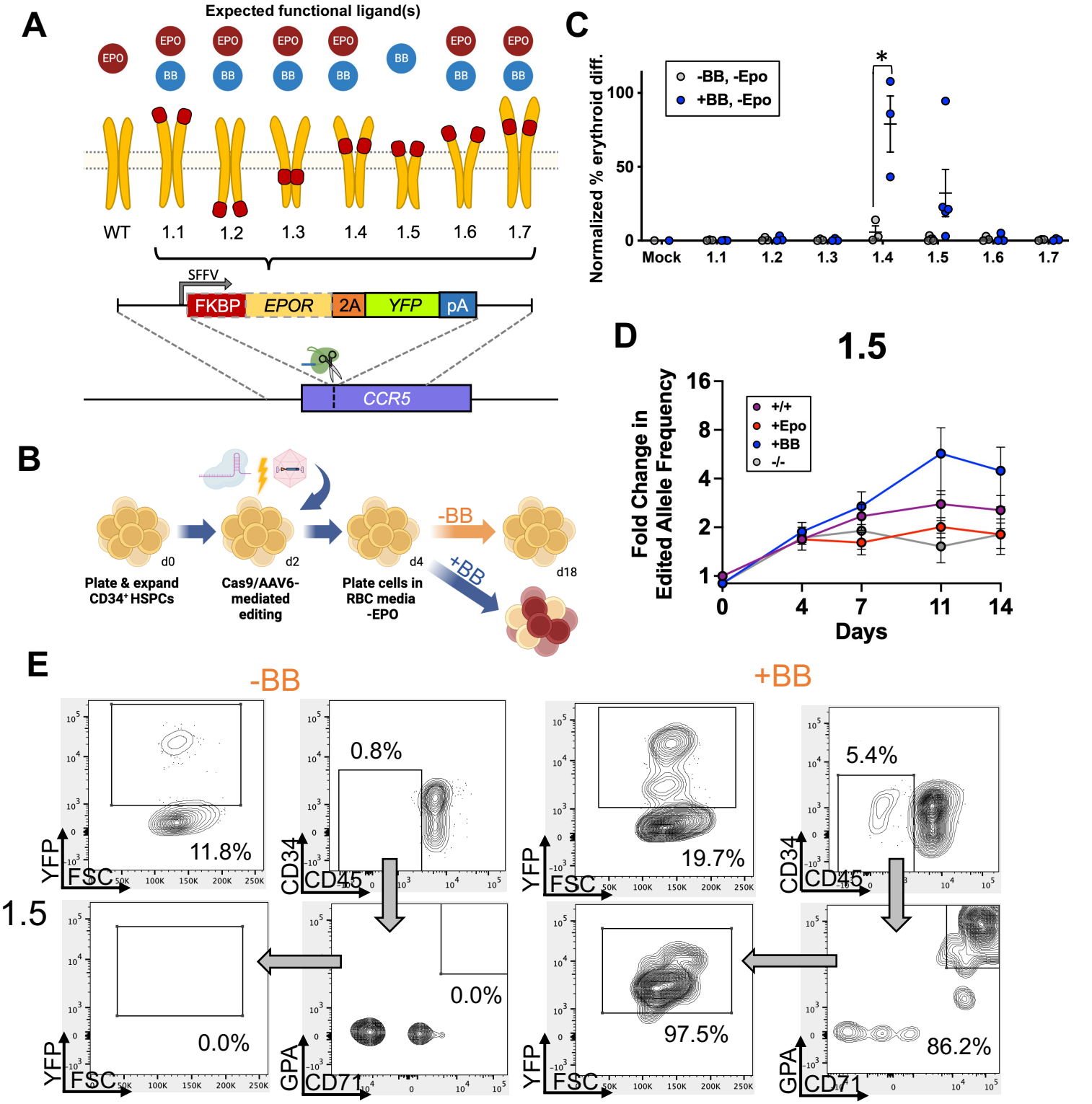

Figure 1. Screening of FKBP-EPOR chimeras to facilitate EPO-free erythroid differentiation.

A: Schematic of chimeric FKBP-EPOR transgenes integrated at the *CCR5* locus via CRISPR/AAV-mediated editing. Red boxes represent the location of FKBP within the EPOR.

B: Schematic of HSPC editing and subsequent erythroid differentiation.

C: Percentage of edited HSPCs that acquired erythroid markers ($CD34^-/CD45^-/CD71^+/GPA^+$) +/-BB normalized to unedited cells +EPO at d14 of differentiation. Bars represent median +/-SEM; * = $p<0.05$ by unpaired t-test.

D: Percent edited alleles over the course of differentiation +/-BB and +/-EPO. Bars represent median +/-SEM.

E: Representative flow cytometry staining and gating scheme for iEPOR 1.5-edited HSPCs at d14 of differentiation -EPO and +/-BB. Arrows indicate that only gated cells are displayed on the subsequent plot.

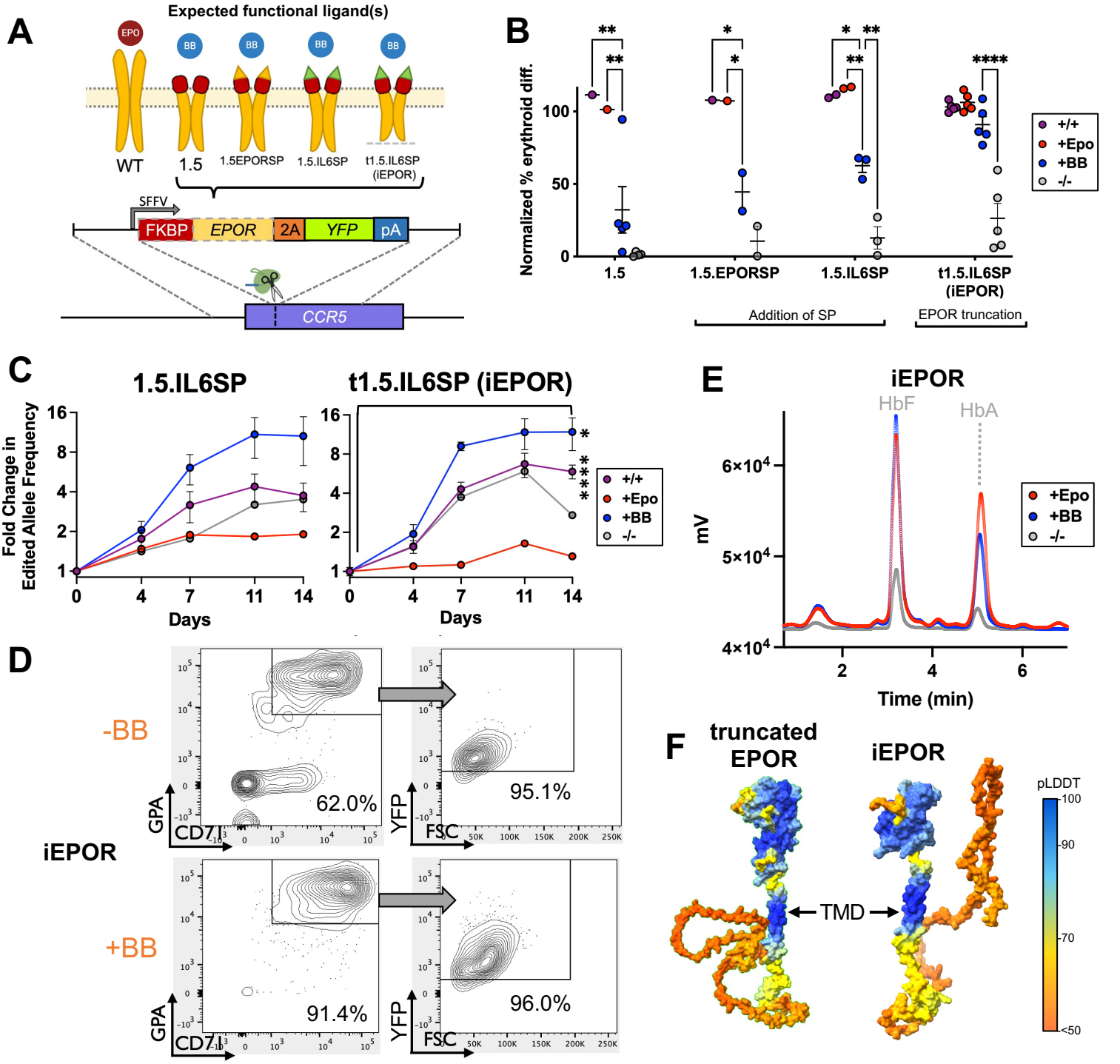

Figure 2: Modulation of iEPOR effect by addition of signal peptide & EPOR truncation.

A: Schematic of second-generation iEPORs integrated at *CCR5* locus. Red boxes represent the FKBP domain; yellow and green triangles indicate EPOR and IL6 SPs, respectively; dashed line represents EPOR truncation.

B: Percentage of edited HSPCs that acquired erythroid markers ($CD34^-/CD45^-/CD71^+/GPA^+$) +/-BB normalized to unedited cells +EPO at d14 of differentiation. iEPOR 1.5 data from Fig. 1C shown for comparison. Bars represent median +/-SEM; * = p<0.05, ** = p<0.01, and **** = p<0.0001 by unpaired t-test.

C: Percent edited alleles over the course of differentiation +/-BB and +/-EPO. Bars represent median +/-SEM; * = p<0.05 and **** = p<0.0001 comparing d0 vs. d14 within treatment by unpaired t-test.

D: Representative flow cytometry staining and gating scheme for iEPOR-edited HSPCs at d14 of differentiation -EPO and +/-BB. Arrows indicate that only gated cells are displayed on the subsequent plot.

E: Representative hemoglobin tetramer HPLC plots at d14 of erythroid differentiation. +BB and -BB/-EPO conditions were from cells edited with iEPOR; +EPO condition was from unedited cells. All plots normalized to 1e6 cells.

F: AlphaFold2-based structure prediction of truncated EPOR and iEPOR. SP was removed since this sequence will be cleaved following translocation to the membrane. TMD labeled with an arrow as a reference point.

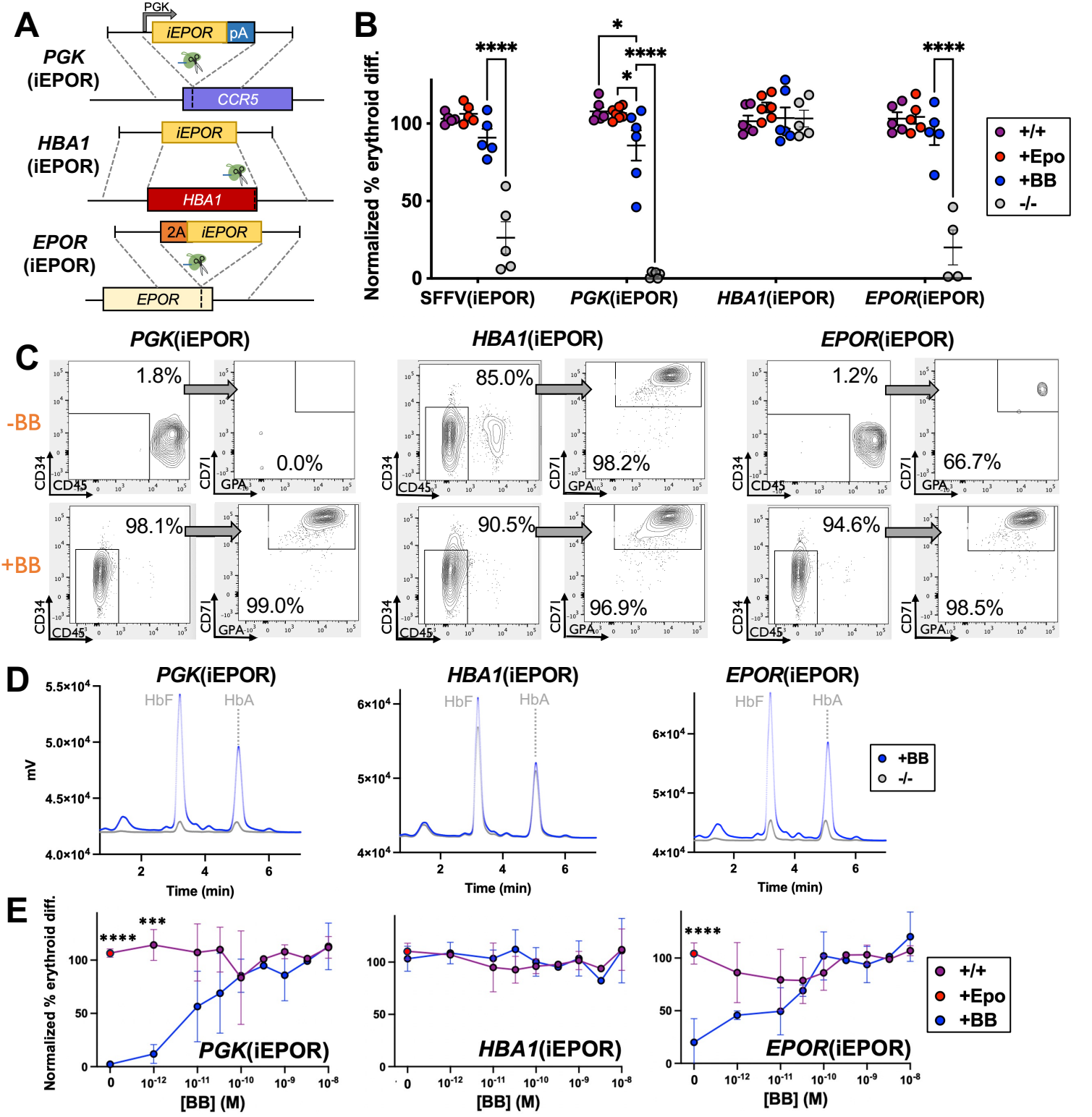

Figure 3: Modulation of iEPOR effect by expression from various promoters.

A Schematic of third-generation iEPORs that drive expression from: 1) PGK promoter from *CCR5* safe harbor site; 2) erythroid-specific *HBA1* locus; and 3) endogenous *EPOR* locus.

B: Percentage of edited HSPCs that acquired erythroid markers ($CD34^-/CD45^-/CD71^+/GPA^+$) +/-BB normalized to unedited cells +EPO at d14 of differentiation. SFFV(iEPOR) data from Fig. 2B shown here for comparison. Bars represent median +/-SEM; * = $p<0.05$, and **** = $p<0.0001$ by unpaired t-test.

C: Representative flow cytometry staining and gating scheme for edited HSPCs at d14 of differentiation -EPO and +/-BB. Arrows indicate that only gated cells are displayed on the subsequent plot.

D: Representative hemoglobin tetramer HPLC plot of edited HSPCs at d14 of differentiation -EPO and +/-BB.

E: Dose response of edited HSPCs cultured over a range of [BB] at d14 of differentiation normalized to unedited cells +EPO. Bars represent median +/-SEM; *** = $p<0.001$ and **** = $p<0.0001$ comparing +EPO/+BB to +BB conditions by unpaired t-test.

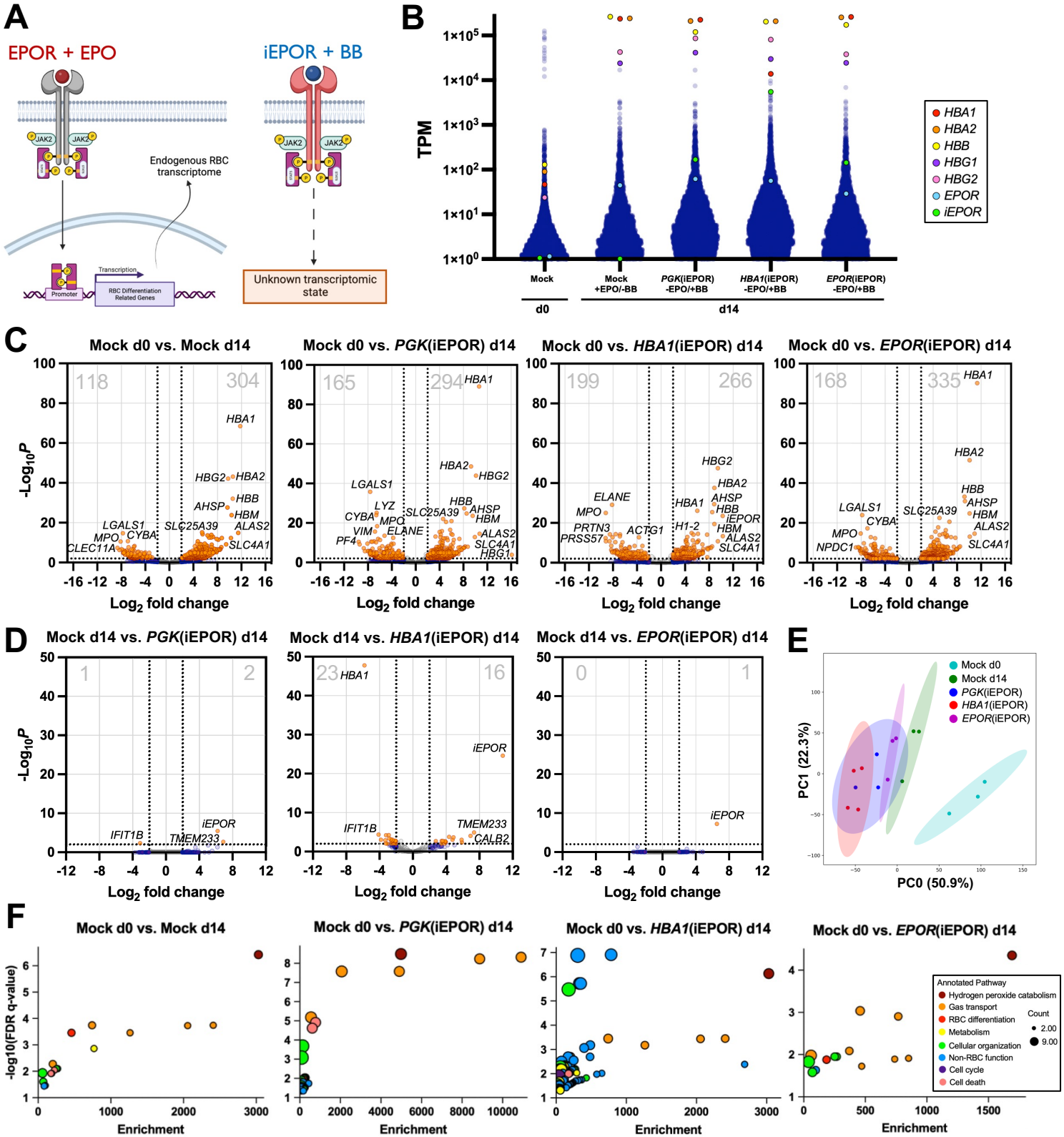

Figure 4: Transcriptome-wide comparison of iEPOR-edited cells to EPO-differentiated cells.

A: Schematic of well-characterized native EPO+EPOR signaling effects vs. undefined BB+iEPOR signaling effects.

B: Transcripts per million (TPM) from RNA-Seq with annotation for globin, *EPOR*, and *iEPOR* genes.

C: Volcano plot comparing unedited and edited HSPCs at d14 of differentiation vs. unedited HSPCs at d0. Dashed lines are drawn at +/-2 $\log_2$ fold change and p=0.01. Total number of significantly down- and upregulated genes is shown in top left and top right of each plot, respectively.

D: Volcano plot comparing edited HSPCs at d14 +BB vs. unedited HSPCs at d14 +EPO. Dashed lines are drawn at +/-2 $\log_2$ fold change and p=0.01. Total number of significantly down- and upregulated genes is shown in top left and top right of each plot, respectively.

E: Principal component analysis of all conditions with covariance ellipses.

F: Summary of gene ontology (GO) analysis comparing all d14 conditions vs. d0 control. Differentially expressed genes from volcano plots (Fig. 4C) were used as input. Specific GO pathways were binned into broader categories and enrichment score was derived by Enrichr software. Count refers to the number of genes within each GO pathway that contributed to enrichment.

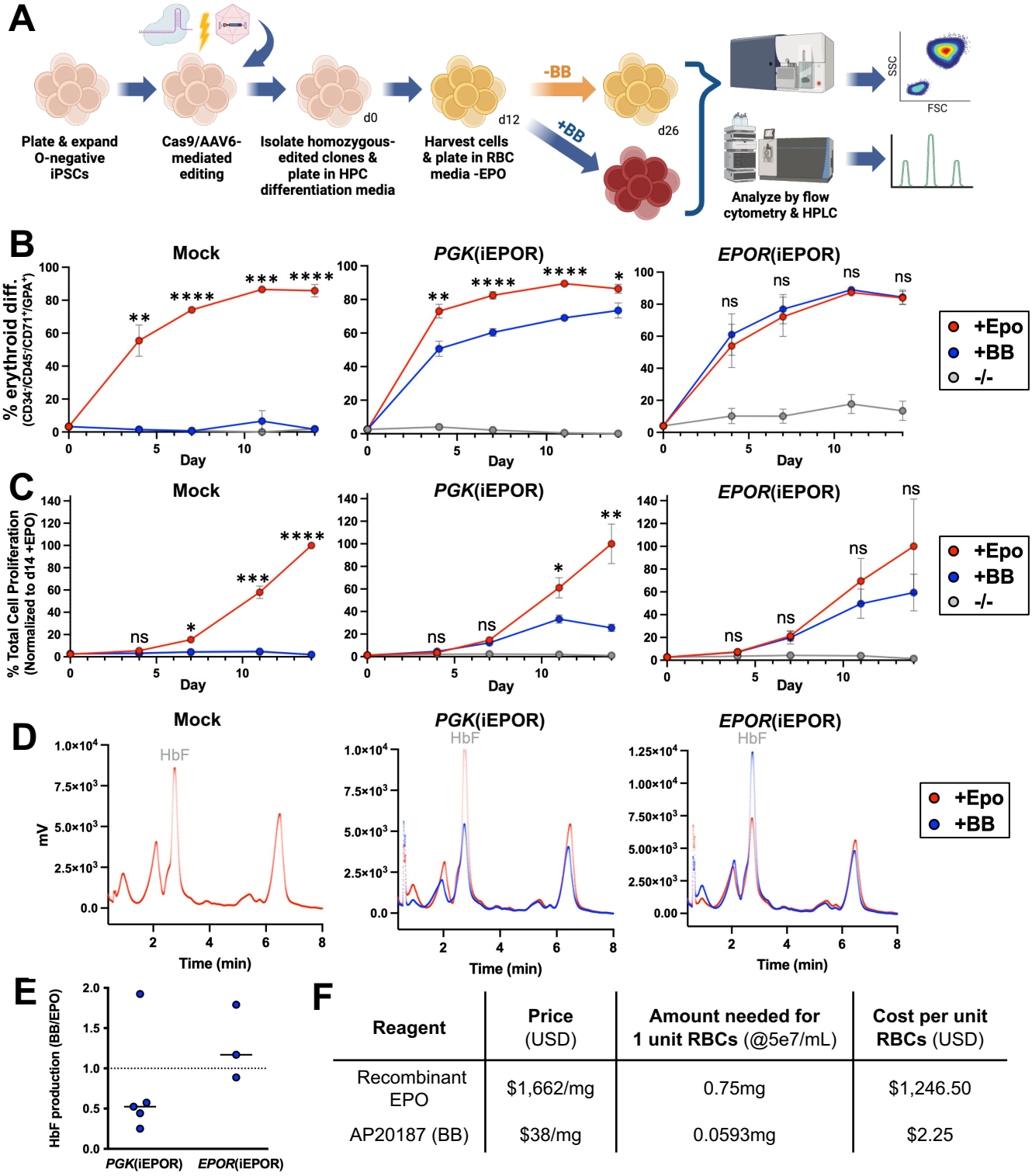

F

Reagent	Price (USD)	Amount needed for 1 unit RBCs (@5e7/mL)	Cost per unit RBCs (USD)
Recombinant EPO	$1,662/mg	0.75mg	$1,246.50
AP20187 (BB)	$38/mg	0.0593mg	$2.25

Figure 5: Differentiation of iPSCs into erythroid cells using iEPOR+BB compared to exogenous EPO.

A: Schematic of iPSC-to-erythroid cell differentiation strategy and subsequent analysis.

B: Percentage of cells that acquired erythroid markers ($CD34^-/CD45^-/CD71^+/GPA^+$) over the course of differentiation. Bars represent mean +/-SEM; ns = not statistically significant, * = p<0.05, ** = p<0.01, *** = p<0.001, and **** = p<0.0001 comparing +BB to +EPO conditions by unpaired t-test.

C: Percentage of total cell proliferation normalized to clones cultured +EPO over the course of differentiation. Bars represent mean +/SEM; ns = not statistically significant, * = p<0.05, ** = p<0.01, *** = p<0.001, and **** = p<0.0001 comparing +BB to +EPO conditions by unpaired t-test.

D: Representative hemoglobin tetramer HPLC plots of edited and unedited iPSC-derived erythroid cells at end of differentiation.

E: Ratio of HbF production in +BB vs. +EPO conditions of iEPOR-edited iPSC-derived erythroid cells at end of differentiation.

F: Cost comparison of EPO and BB (lowest price per mg commercially available for purchase as of 2/9/24).